

# Computer simulation of the thermodynamic properties of high-temperature chemically-reacting plasmas

Martin Lísal

*E. Hála Laboratory of Thermodynamics, Institute of Chemical Process Fundamentals, Academy of Sciences, 165 02 Prague 6, Czech Republic and Department of Mathematics and Statistics and School of Engineering, College of Physical and Engineering Science, University of Guelph, Guelph, Ontario N1G 2W1, Canada*

William R. Smith

*Department of Mathematics and Statistics, and School of Engineering, College of Physical and Engineering Science, University of Guelph, Guelph, Ontario N1G 2W1, Canada*

Ivo Nezbeda

*E. Hála Laboratory of Thermodynamics, Institute of Chemical Process Fundamentals, Academy of Sciences, 165 02 Prague 6, Czech Republic and Department of Physics, J. E. Purkyně University, 400 96 Ustí n. Lab., Czech Republic*

(Received 12 April 2000; accepted 26 June 2000)

The Reaction Ensemble Monte Carlo (REMC) computer simulation method [W. R. Smith and B. Tříska, *J. Chem. Phys.* **100**, 3019 (1994)] is employed to predict the thermodynamic behavior of chemically reacting plasmas using a molecular-level model based on the underlying atomic and ionic interactions. Unlike previous plasma simulation studies, which were restricted to fairly simple systems of fixed composition, the REMC approach is able to take into account the effects of the ionization reactions. In the context of the specified molecular model, the computer simulation approach gives an essentially exact description of the system thermodynamics. We develop and apply the REMC method for the test case of a helium plasma. We calculate plasma compositions, molar enthalpies, molar volumes, molar heat capacities, and coefficients of cubic expansion over a range of temperatures up to 100 000 K and pressures up to 400 MPa. We elucidate the contributions of the Coulombic forces, ionization-potential lowering, and short-ranged interactions to the thermodynamic properties. We compare the results with those obtained using macroscopic-level thermodynamic approximations, including the ideal-gas (IG) and the Debye–Hückel (DH) approaches. For the helium plasma, the short-ranged forces are found to be relatively unimportant, but we expect these to be important for molecular systems. The DH theory is always more accurate than the IG approximation. The DH theory yields compositions that slightly underpredict the overall degree of ionization. For the molar heat capacity and the coefficient of cubic expansion, the DH theory is accurate at lower pressures, but at 400 MPa yields results that are up to 40% in error for the molar heat capacity. © 2000 American Institute of Physics. [S0021-9606(00)50236-0]

## I. INTRODUCTION

The plasma state is frequently referred to as the fourth state of matter in the sequence: solid, liquid, gas, *plasma*. Plasmas are important in materials processing, including melting and refining of metals and alloys, plasma chemical synthesis, and plasma waste destruction. Other important applications occur in high-voltage circuit breakers, nuclear reactors, and electrical discharge machines. Temperatures of interest in plasmas range up to 100 000 K, and pressures up to 100 MPa or more.<sup>1,2</sup>

Among the most important properties of a plasma are its composition and its thermodynamic and transport properties. Most plasma models employ as a basic assumption the condition of *local chemical equilibrium*. This means that the electrons, ions, and neutral particles all have the same (kinetic) temperature and that reaction chemical equilibrium has been achieved locally.<sup>1</sup> Chemical equilibrium at specified temperature  $T$  and pressure  $P$  is attained when the system

Gibbs free energy is minimized subject to the mass conservation, charge neutrality and non-negativity constraints.<sup>3</sup>

At the macroscopic (thermodynamic) level, specification of the system Gibbs free energy entails modeling of the species chemical potentials, and its minimization requires the use of a nonlinear optimization algorithm. The chemical potential of each species is the sum of an ideal contribution and a nonideal (excess) contribution. Sources of nonideality in plasmas are the presence of long-ranged Coulombic interactions between charged particles, the composition-dependent lowering of the ionization potential, and short-ranged (neutral–neutral and neutral–charged particle) interactions. Traditionally, only the first two factors have been taken into account, both using the Debye–Hückel (DH) approximate theory.<sup>1</sup> The numerical calculation of plasma compositions by means of the macroscopic approach remains an active area of interest.<sup>2,4–6</sup>

Molecular-level computer simulation techniques provide, in principle, a computational tool for the essentially

exact calculation of macroscopic plasma properties based on only a knowledge of the underlying intermolecular potential models. Previous simulation methods for plasmas (for a review, see e.g., Hansen<sup>7</sup>) have been limited in their ability to realistically model plasma behavior due to their inability to account for the ionization reactions. They focused mainly on the interactions between the charged particles, and studies were carried out only on relatively simple systems of fixed composition. In addition no comparisons were generally made with results of approximate theories.

The recently-developed Reaction Ensemble Monte Carlo (REMC) method, due to Smith and Trřiska,<sup>8</sup> is a molecular-level simulation method for calculating equilibrium compositions and thermodynamic properties of systems undergoing an arbitrary number of chemical reactions and consisting of any number of phases. It has been shown to be a useful tool for predicting the chemical and phase equilibria of systems encountered in the chemical processing industry.<sup>9–11</sup> Its potential uses and limitations are discussed in the original paper.<sup>8</sup>

The purpose of this paper is to demonstrate the application of the REMC computer simulation method to predict the behavior of chemically-reacting plasmas. Such systems are qualitatively different from those typically encountered in the chemical processing industry, due to the presence of ionic forces and high temperatures and pressures. We develop the required simulation formulation, and consider the helium plasma as a test case. For this system, we assess the accuracy of the classical DH macroscopic model, and also consider the contributions of different aspects of the molecular-level model [Coulombic forces, ionization-potential (IP) lowering, and short-ranged interactions] to the plasma properties.

In the next two sections of the paper, we describe the details of the REMC methodology for the helium plasma; this is followed by a description of the intermolecular potential models used. The subsequent section describes the details of the simulations, followed by a section concerning results and their discussion. The final section contains our conclusions.

## II. REMC SIMULATION METHODOLOGY FOR THE HELIUM PLASMA

The helium plasma is a reacting mixture involving the four species: neutral He(1), ions He<sup>+</sup>(2), and He<sup>++</sup>(3), and electrons e<sup>-</sup>(4), which is governed by the ionization reactions



The *reaction ensemble partition function*<sup>8</sup> for this system can be written as

$$\begin{aligned} Q(N_1, \dots, N_4, P, T) &= \sum_{\xi_1} \sum_{\xi_2} \prod_i \frac{(Vq_i/\Lambda_i^3)^{(N_i^0 + \sum_j \xi_j \nu_{ji})}}{(N_i^0 + \sum_j \xi_j \nu_{ji})!} \\ &\times \int \exp\{-\beta[U(V, \mathbf{z}_1, \dots, \mathbf{z}_N) + PV]\} d\mathbf{z}_1, \dots, d\mathbf{z}_N, \end{aligned} \quad (2.3)$$

where  $V$  is the system volume,  $q_i$  is the internal part of the partition function for species  $i$  ( $i=1,2,3,4$ ), and  $\Lambda_i$  is its de Broglie thermal wavelength.  $N_i$  is the number of particles of species  $i$ , and  $\{N_i^0\}$  represents an arbitrary particular system composition satisfying the mass-balance and charge-neutrality constraints.  $\xi_1$  and  $\xi_2$  are reaction extents for reactions (2.1) and (2.2), respectively,  $\nu_{ji}$  are the stoichiometric coefficients corresponding to these reactions,  $U(V, \mathbf{z}_1, \dots, \mathbf{z}_N)$  is the configurational energy expressed in terms of  $V$  and the scaled variables  $\mathbf{z}$  which lie in (0,1), and  $\beta = 1/(k_B T)$ , where  $k_B$  is Boltzmann's constant. The summations are over all (integral) values of  $\xi_1$  and  $\xi_2$  for which the particle amounts  $N_i = N_i^0 + \sum_j \xi_j \nu_{ji}$  remain non-negative.

The REMC method generates a Markov chain to simulate the properties of a system governed by Eq. (2.3). The chain consists of three types of state transitions: particle moves, volume changes and reaction moves. The particle moves and volume changes are implemented in the usual way;<sup>12</sup> the transition probability  $k \rightarrow l$  for particle moves is

$$P_{kl}^D = \min[1, \exp(-\beta \Delta U_{kl})], \quad (2.4)$$

where  $\Delta U_{kl} = U_l - U_k$  is the change in configurational energy. The transition probability  $k \rightarrow l$  for volume changes is

$$P_{kl}^V = \min\left\{1, \exp\left[-\beta \Delta U_{kl} - \beta P(V_l - V_k) + N \ln \frac{V_l}{V_k}\right]\right\}. \quad (2.5)$$

The transition probability  $k \rightarrow l$  for reaction moves  $\xi$  for reaction  $j$  is<sup>8</sup>

$$P_{j,kl}^\xi = \min\left\{1, V^{\bar{\nu}_j \xi} \Gamma_j^\xi \prod_i \left[\frac{(N_i^0)!}{(N_i^0 + \nu_{ji} \xi)!}\right] \exp(-\beta \Delta U_{kl})\right\}, \quad (2.6)$$

where  $\bar{\nu}_j$  is the net change in the number of moles for reaction  $j$ ,  $\bar{\nu}_j = \sum_i \nu_{ji}$ , and  $\Gamma_j$  is the ideal-gas (IG) driving force for the reaction,

$$\Gamma_j = \exp\left[-\frac{\sum_i \nu_{ji} \mu_i^0(T, P^0)}{RT}\right] \left(\frac{P^0}{k_B T}\right)^{\bar{\nu}_j}, \quad (2.7)$$

where  $\mu_i^0(T, P^0)$  is the molar standard chemical potential of species  $i$  at the temperature  $T$  and the standard-state pressure  $P^0$  (taken to be 1 bar), and  $R$  is the universal gas constant.

In the particular case of the helium plasma considered here, for reaction (2.1), the transition probability  $k \rightarrow l$  for a forward reaction move ( $\xi = +1$ ) is

$$P_{1,kl}^{+1} = \min\left[1, V \Gamma_1 \frac{N_1}{(N_2 + 1)(N_4 + 1)} \exp(-\beta \Delta U_{kl})\right] \quad (2.8)$$

and the transition probability  $k \rightarrow l$  for a reverse reaction move ( $\xi = -1$ ) is

$$P_{1,kl}^{-1} = \min \left[ 1, \frac{1}{\sqrt{\Gamma_1}} \frac{N_2 N_4}{N_1 + 1} \exp(-\beta \Delta U_{kl}) \right]. \quad (2.9)$$

The transition probabilities for reaction (2.2) are given by similar expressions.

Reaction steps for reactions (2.1) and (2.2) are carried out as follows: (i) a reaction is selected randomly with equal probability, and (ii) for the selected reaction, a forward or reverse reaction move is attempted according to a preset probability of 0.5. For a forward move, a reactant particle  $A$  is selected at random, and an attempt is made to simultaneously replace it by a product particle  $B$  and to insert a product particle  $C$  at a random position in the system. Similarly, for a reverse move, product particles  $B$  and  $C$  are chosen at random, and an attempt is made to simultaneously replace the  $B$  particle by a reactant particle  $A$  and to delete the  $C$  particle. Equations (2.8) and (2.9) give the respective probabilities of success of each type of reaction move.

### III. CALCULATION OF $\mu^0(T, P^0)$ AND THE INCORPORATION OF IONIZATION-POTENTIAL LOWERING

The dependence of  $\mu_i^0(T, P^0)$  on  $P^0$  is usually suppressed, and  $\mu_i^0(T)$  may be expressed as

$$\mu_i^0(T) = h_i^0(T) - T s_i^0(T), \quad (3.1)$$

where the molar enthalpy  $h_i^0(T)$  and the molar entropy  $s_i^0(T)$  may be expressed as

$$h_i^0(T) = \Delta H_{fi}(T_r) + \int_{T_r}^T c_{pi}^0(T) dT, \quad (3.2)$$

$$s_i^0(T) = s_i^0(T_r) + \int_{T_r}^T \frac{c_{pi}^0(T)}{T} dT. \quad (3.3)$$

In Eqs. (3.2) and (3.3),  $\Delta H_{fi}(T_r)$  is the enthalpy of formation of species  $i$  at the reference temperature  $T_r$  (taken here as 298.15 K);  $s_i^0(0) \equiv 0$ , and  $c_{pi}^0(T)$  is the IG heat capacity of species  $i$ .  $c_{pi}^0$  are obtained by appropriate summations over the energy levels of species  $i$ .<sup>13</sup>  $\Delta H_{fi}$  are determined from IP data [the enthalpy changes  $IP_1$  and  $IP_2$  for reactions (2.1) and (2.2), respectively, at 0 K] and heat-capacity data; adopting the convention that  $\Delta H_{fi}(T_r) \equiv 0$  for He and for  $e^-$  gives

$$\begin{aligned} \Delta H_{f, \text{He}^+}(T_r) = & IP_1 + \int_0^{T_r} [c_{p, \text{He}^+}^0(T) \\ & + c_{p, e^-}^0(T) - c_{p, \text{He}}^0(T)] dT, \end{aligned} \quad (3.4)$$

$$\begin{aligned} \Delta H_{f, \text{He}^{++}}(T_r) = & IP_1 + IP_2 + \int_0^{T_r} [c_{p, \text{He}^{++}}^0(T) \\ & + c_{p, e^-}^0(T) - c_{p, \text{He}^+}^0(T)] dT. \end{aligned} \quad (3.5)$$

In a plasma, the Coulombic interactions lower  $IP_i$ .<sup>1,2,6</sup> The exact calculation of this effect is a complex problem.<sup>14</sup> The essential difficulty is that the internal and configurational parts of the partition function are not independent. Any suitable approximation for this effect may be incorporated into the REMC simulation methodology, in principle.

For the calculations of this paper, we incorporate a typically-used approximation, obtained from the correction of the Saha equation<sup>15,16</sup>

$$\Delta I_z = \frac{z e^2 N_A}{4 \pi \epsilon_0 \lambda_D}, \quad (3.6)$$

where  $z$  is the ionic charge of the product ion,  $e$  is the electronic charge,  $\epsilon_0$  is the permittivity of free space,  $N_A$  is Avogadro's number, and  $\lambda_D$  is the Debye length, defined by

$$\lambda_D = \left( \frac{v \epsilon_0 k_B T}{e^2 N_A \sum_i y_i z_i^2} \right)^{1/2}, \quad (3.7)$$

where  $v$  is the molar volume and  $y_i$  is the mole fraction of species  $i$ . Equation (3.6) may be used for densities fulfilling the inequality<sup>15</sup>

$$6 \left( \frac{\lambda_D}{a} \right)^3 \geq 1, \quad (3.8)$$

where  $a$  is the mean particle spacing,

$$a = \left( \frac{3v}{4\pi N_A} \right)^{1/3}. \quad (3.9)$$

The IP lowering directly affects  $\Delta H_f(T_r)$  for the ionic species by the lowered  $IP_1$  and  $IP_2$  values in Eqs. (3.4) and (3.5). It also has a secondary effect on  $h_i^0(T)$ ,  $s_i^0(T)$ , and  $\mu_i^0(T)$  for the ions via its effect on the  $c_{pi}^0$  values, resulting from the lowering of the upper energy limit (the ionization limit) in the partition function summations used in their calculation. If we neglect the latter effect, the IP lowering may be incorporated into a modification of the molar enthalpy for an ionic species of charge  $+z$ .<sup>2,6,17</sup> The molar enthalpy of an ion  $A^{+z}$ ,  $h_{A^{+z}}^0(T)$ , is modified to

$$h_{A^{+z}}^0(T) = \tilde{h}_{A^{+z}}^0(T) - \frac{z(z+1)}{2} \frac{e^2 N_A}{4\pi\epsilon_0\lambda_D}, \quad (3.10)$$

where  $\tilde{h}_{A^{+z}}^0(T)$  is computed from Eq. (3.2). The final expression for  $\mu_i^0(T)$  is obtained by using Eq. (3.10) in conjunction with Eqs. (3.1)–(3.3).

Numerical values of  $\Delta H_{fi}(298.15)$ ,  $s_i^0(298.15)$ , and coefficients  $a_1$ – $a_5$  of a piecewise polynomial expression for  $c_{pi}^0$ ,

$$c_{pi}^0 = a_{1i} + (a_{2i} + a_{3i}T)T + \left( a_{4i} + \frac{a_{5i}}{T} \right) \frac{1}{T} \quad (3.11)$$

for the species in the helium plasma are listed in Table I. These were obtained by calculations involving the energy levels<sup>18</sup> and least squares fits to the resulting values over the temperature range 298.15 K–100 000 K.<sup>6</sup>

Since the species chemical potentials are affected, the IP lowering also makes a contribution to the system pressure, given by<sup>6,17</sup>

$$\begin{aligned} P^{\text{IPL}} = & - \frac{e^2 N_A}{24\pi\epsilon_0 v \lambda_D} \sum_{z_i > 0} y_i z_i (z_i + 1) \\ = & - \frac{e^2 N_A}{24\pi\epsilon_0 v \lambda_D} (2y_2 + 6y_3). \end{aligned} \quad (3.12)$$

TABLE I. The enthalpy of formation,  $\Delta H_f(298.15)$ , and the molar entropy,  $s^0(298.15)$ , and coefficients  $a_1$ – $a_5$  of the piecewise polynomial expression over the temperature intervals  $T_{\min}$ – $T_{\max}$  for the ideal-gas heat capacity  $c_p^0$ , Eq. (3.11), for He, He<sup>+</sup>, He<sup>++</sup>, and e<sup>−</sup>.

Component	$\Delta H_f(298.15)$ (kJ mol <sup>−1</sup> )	$s^0(298.15)$ (J mol <sup>−1</sup> K <sup>−1</sup> )	$T_{\min.}$ (K)	$T_{\max}$ (K)	$a_1$ (J mol <sup>−1</sup> K <sup>−1</sup> )	$a_2$ (J mol <sup>−1</sup> K <sup>−2</sup> )
He	0	126.142 54	298.15	5000	20.788 48	$-1.014\,081 \cdot 10^{-6}$
			5000	13 000	20.048 05	$6.002\,115 \cdot 10^{-5}$
			13 000	24 000	69.288 24	$-2.485\,508 \cdot 10^{-3}$
			24 000	40 000	$-57.168\,55$	$9.290\,289 \cdot 10^{-4}$
			40 000	100 000	1127.019	$-1.287\,236 \cdot 10^{-2}$
He <sup>+</sup>	2378.521	131.903 99	298.15	5000	20.788 48	$-1.014\,081 \cdot 10^{-6}$
			5000	13 000	23.284 93	$-2.010\,410 \cdot 10^{-4}$
			13 000	24 000	$-177.3043$	$7.396\,548 \cdot 10^{-3}$
			24 000	40 000	110.2072	$-2.046\,241 \cdot 10^{-3}$
			40 000	100 000	$-766.8953$	$7.795\,158 \cdot 10^{-3}$
He <sup>++</sup>	7635.234	126.022 52	298.15	100 000	20.786 00	0
e <sup>−</sup>	0	20.979 00	298.15	100 000	20.786 00	0

Component	$a_3$ (J mol <sup>−1</sup> K <sup>−3</sup> )	$a_4$ (J mol <sup>−1</sup> )	$a_5$ (J K mol <sup>−1</sup> )
He	$1.276\,923 \cdot 10^{-10}$	$-0.159\,432\,7 \cdot 10^1$	$3.030\,149 \cdot 10^2$
	$-1.763\,19 \cdot 10^{-9}$	$3.884\,011 \cdot 10^3$	$-7.384\,388 \cdot 10^6$
	$4.670\,972 \cdot 10^{-8}$	$-4.073\,897 \cdot 10^5$	$1.224\,357 \cdot 10^9$
	$2.101\,506 \cdot 10^{-8}$	$1.121\,259 \cdot 10^6$	$-1.244\,362 \cdot 10^9$
	$5.012\,162 \cdot 10^{-8}$	$-3.420\,083 \cdot 10^7$	$3.245\,554 \cdot 10^{11}$
He <sup>+</sup>	$1.276\,923 \cdot 10^{-10}$	$-0.159\,432\,7 \cdot 10^1$	$3.030\,149 \cdot 10^2$
	$5.854\,660 \cdot 10^{-9}$	$-1.330\,065 \cdot 10^4$	$2.557\,960 \cdot 10^7$
	$-1.020\,674 \cdot 10^{-7}$	$2.323\,517 \cdot 10^6$	$-1.007\,230 \cdot 10^{10}$
	$1.739\,985 \cdot 10^{-8}$	$-1.719\,930 \cdot 10^6$	$1.228\,263 \cdot 10^{10}$
	$-2.265\,154 \cdot 10^{-8}$	$3.184\,560 \cdot 10^7$	$-4.546\,818 \cdot 10^{11}$
He <sup>++</sup>	0	0	0
e <sup>−</sup>	0	0	0

## IV. INTERMOLECULAR POTENTIAL MODELS

### A. Charged particle-charged particle interactions

The typical range of temperatures and pressures in plasma applications is such that the reduced de Broglie thermal wavelength of electrons is shorter than the mean interparticle distance, and hence, the electrons may be treated as only *weakly degenerate*.<sup>7</sup> The interactions between charged particles in the helium plasma [He<sup>+</sup>(2), He<sup>++</sup>(3), e<sup>−</sup>(4)] can then be described by effective pair potentials, as given by Deutsch and co-workers<sup>19</sup> in the form

$$u_{ab} = \frac{z_a z_b e^2}{4\pi\epsilon_0 r} \left[ 1 - \exp\left(-\frac{r}{R_{ab}}\right) \right] + \delta_{a4} \delta_{b4} u_{44}^{(s)}. \quad (4.1)$$

In Eq. (4.1),  $r$  is the distance between particles  $a$  and  $b$ ,  $R_{ab}^2 = \bar{\Lambda}_a^2 + \bar{\Lambda}_b^2$ , where  $\bar{\Lambda}_a$  and  $\bar{\Lambda}_b$  are the reduced de Broglie thermal wavelengths of particles  $a$  and  $b$ , given by  $\bar{\Lambda} = \hbar / \sqrt{2\pi m k_B T}$ , where  $\hbar$  is the reduced Planck constant and  $m$  is the particle mass. Finally,  $\delta$  is the Kronecker delta. The term  $u_{44}^{(s)}$  accounts for the electron symmetry effect and is given as

$$u_{44}^{(s)} = k_B T \ln 2 \cdot \exp\left[-\frac{1}{\pi \ln 2} \left(\frac{r}{R_{44}}\right)^2\right]. \quad (4.2)$$

### B. Neutral particle–neutral particle interactions

The interactions between neutral particles in the helium plasma [He(1)] were represented by the exponential-6 (Exp-6) potential

$$u_{11}(r) = \infty, \quad r < r_c \\ = A \exp(-Br) - C_6 r^{-6}, \quad r \geq r_c, \quad (4.3)$$

where  $r_c$  is the range of the Exp-6 core, and the Exp-6 coefficients  $A$ ,  $B$ , and  $C_6$  are defined using the attractive well-depth  $\epsilon$ , the range of the exponential repulsion  $r_m$  and the stiffness parameter of the exponential repulsion  $\zeta$  as

$$A = \epsilon \frac{6}{\zeta - 6} \exp(\zeta), \quad B = \frac{\zeta}{r_m}, \quad C_6 = \epsilon \frac{\zeta}{\zeta - 6} r_m^6. \quad (4.4)$$

Numerical values of the Exp-6 potential parameters for the He–He interactions were taken from Ree<sup>20</sup> and are listed in Table II.

TABLE II. Coefficients of  $A$ ,  $B$ , and  $C_6$ , and the range of the potential core  $r_c$  of the Exp-6 potentials for the He–He and He–He<sup>+</sup> interactions employed in the present work.

	$A$ (J)	$B$ (m <sup>−1</sup> )	$C_6$ (J m <sup>6</sup> )	$r_c$ (m)
He–He <sup>20</sup>	$6.161 \cdot 10^{-17}$	$4.4148 \cdot 10^{-10}$	$1.878 \cdot 10^{-79}$	$0.7185 \cdot 10^{-10}$
He–He <sup>+</sup>	$6.161 \cdot 10^{-17}$	$5.2802 \cdot 10^{-10}$	$0.642 \cdot 10^{-79}$	$0.6008 \cdot 10^{-10}$

TABLE III. The excess molar internal energy  $u^e$ , molar volume  $v$ , mole fractions  $\{y_{\text{He}}, y_{\text{He}^+}, y_{\text{He}^{++}}, y_{e^-}\}$ , and the number of moles per total molar amount of He,  $n_t$ , for the helium plasma at  $P = 10$  MPa from the Reaction Ensemble Monte Carlo simulations of this work. The simulation uncertainties are given in the last digits as subscripts. The last column gives the left-hand side of Eq. (3.8).

$T$ (K)	$u^e$ (kJ mol $^{-1}$ )	$v$ (m $^3$ mol $^{-1}$ )	$y_{\text{He}}$	$y_{\text{He}^+}$	$y_{\text{He}^{++}}$	$y_{e^-}$	$n_t$	$6\left(\frac{\lambda_D}{a}\right)^3$
20 000	-3.39 <sub>188</sub>	0.016 69 <sub>35</sub>	0.9477 <sub>11</sub>	0.0231 <sub>6</sub>	0.0020 <sub>0</sub>	0.0272 <sub>6</sub>	1.028 <sub>1</sub>	276.28
22 500	-5.64 <sub>197</sub>	0.018 62 <sub>15</sub>	0.8719 <sub>11</sub>	0.0611 <sub>6</sub>	0.0020 <sub>0</sub>	0.0650 <sub>6</sub>	1.070 <sub>1</sub>	99.82
25 000	-10.64 <sub>239</sub>	0.020 43 <sub>23</sub>	0.7436 <sub>16</sub>	0.1254 <sub>8</sub>	0.0019 <sub>0</sub>	0.1291 <sub>18</sub>	1.149 <sub>1</sub>	44.82
27 500	-18.42 <sub>221</sub>	0.022 14 <sub>37</sub>	0.5725 <sub>26</sub>	0.2113 <sub>13</sub>	0.0016 <sub>0</sub>	0.2146 <sub>13</sub>	1.273 <sub>2</sub>	25.41
30 000	-25.08 <sub>213</sub>	0.023 85 <sub>17</sub>	0.3958 <sub>18</sub>	0.2999 <sub>9</sub>	0.0015 <sub>0</sub>	0.3028 <sub>9</sub>	1.435 <sub>2</sub>	17.98
32 500	-30.65 <sub>171</sub>	0.025 75 <sub>24</sub>	0.2491 <sub>17</sub>	0.3734 <sub>9</sub>	0.0014 <sub>0</sub>	0.3761 <sub>9</sub>	1.603 <sub>2</sub>	15.25
35 000	-32.92 <sub>182</sub>	0.027 63 <sub>32</sub>	0.1495 <sub>14</sub>	0.4234 <sub>7</sub>	0.0012 <sub>0</sub>	0.4259 <sub>7</sub>	1.742 <sub>2</sub>	14.68
37 500	-33.24 <sub>184</sub>	0.029 87 <sub>49</sub>	0.0883 <sub>11</sub>	0.4540 <sub>6</sub>	0.0012 <sub>0</sub>	0.4565 <sub>6</sub>	1.840 <sub>2</sub>	15.25
40 000	-32.15 <sub>138</sub>	0.031 81 <sub>28</sub>	0.0535 <sub>5</sub>	0.4713 <sub>2</sub>	0.0013 <sub>0</sub>	0.4739 <sub>3</sub>	1.901 <sub>1</sub>	16.39
42 500	-30.72 <sub>100</sub>	0.033 98 <sub>47</sub>	0.0333 <sub>4</sub>	0.4810 <sub>2</sub>	0.0015 <sub>1</sub>	0.4842 <sub>2</sub>	1.939 <sub>1</sub>	17.96
45 000	-29.15 <sub>118</sub>	0.036 26 <sub>46</sub>	0.0216 <sub>3</sub>	0.4857 <sub>2</sub>	0.0023 <sub>1</sub>	0.4904 <sub>1</sub>	1.962 <sub>1</sub>	19.78
50 000	-28.39 <sub>151</sub>	0.040 59 <sub>55</sub>	0.0101 <sub>2</sub>	0.4814 <sub>5</sub>	0.0090 <sub>4</sub>	0.4995 <sub>2</sub>	1.998 <sub>1</sub>	23.38
55 000	-30.57 <sub>294</sub>	0.045 40 <sub>96</sub>	0.0052 <sub>2</sub>	0.4512 <sub>10</sub>	0.0308 <sub>7</sub>	0.5128 <sub>4</sub>	2.053 <sub>2</sub>	25.80
60 000	-35.27 <sub>415</sub>	0.048 22 <sub>55</sub>	0.0030 <sub>1</sub>	0.3856 <sub>13</sub>	0.0753 <sub>9</sub>	0.5361 <sub>4</sub>	2.155 <sub>2</sub>	25.40
65 000	-41.47 <sub>417</sub>	0.053 43 <sub>103</sub>	0.0018 <sub>1</sub>	0.2862 <sub>25</sub>	0.1419 <sub>17</sub>	0.5701 <sub>9</sub>	2.326 <sub>5</sub>	24.00
70 000	-44.91 <sub>363</sub>	0.056 30 <sub>71</sub>	0.0012 <sub>0</sub>	0.1918 <sub>15</sub>	0.2051 <sub>10</sub>	0.6019 <sub>5</sub>	2.513 <sub>3</sub>	22.81
75 000	-45.97 <sub>455</sub>	0.061 24 <sub>76</sub>	0.0009 <sub>0</sub>	0.1172 <sub>13</sub>	0.2549 <sub>8</sub>	0.6270 <sub>4</sub>	2.681 <sub>3</sub>	23.10
80 000	-43.92 <sub>257</sub>	0.065 37 <sub>78</sub>	0.0009 <sub>0</sub>	0.0707 <sub>8</sub>	0.2859 <sub>5</sub>	0.6425 <sub>3</sub>	2.798 <sub>2</sub>	24.34
85 000	-43.08 <sub>203</sub>	0.068 43 <sub>186</sub>	0.0008 <sub>0</sub>	0.0437 <sub>6</sub>	0.3039 <sub>4</sub>	0.6516 <sub>2</sub>	2.870 <sub>2</sub>	26.12
90 000	-41.90 <sub>252</sub>	0.072 83 <sub>65</sub>	0.0008 <sub>0</sub>	0.0274 <sub>3</sub>	0.3148 <sub>4</sub>	0.6570 <sub>10</sub>	2.915 <sub>1</sub>	28.62
95 000	-39.60 <sub>207</sub>	0.077 06 <sub>10</sub>	0.0008 <sub>0</sub>	0.0178 <sub>3</sub>	0.3212 <sub>2</sub>	0.6602 <sub>1</sub>	2.943 <sub>0</sub>	31.46
100 000	-36.48 <sub>208</sub>	0.081 73 <sub>135</sub>	0.0007 <sub>0</sub>	0.0120 <sub>2</sub>	0.3251 <sub>2</sub>	0.6622 <sub>1</sub>	2.960 <sub>1</sub>	34.68

### C. Neutral particle-charged particle interactions

The He-He $^+$  interactions were also represented by Exp-6 potentials. To obtain the potential parameters, we used the Universal Force Field approach.<sup>21</sup> This first constructs a

hypothetical Exp-6 potential for He $^+$ -He $^+$  interaction as follows. The potential has the same stiffness parameters as the neutral He atoms, i.e.,  $\zeta_{\text{He}^+} = \zeta_{\text{He}}$ ; the  $B_{\text{He}^+}$  and  $C_{6_{\text{He}^+}}$  Exp-6 coefficients are evaluated by scaling the  $B_{\text{He}}$  and  $C_{6_{\text{He}}}$

TABLE IV. The excess molar internal energy  $u^e$ , molar volume  $v$ , mole fractions  $\{y_{\text{He}}, y_{\text{He}^+}, y_{\text{He}^{++}}, y_{e^-}\}$ , and the number of moles per total molar amount of He,  $n_t$ , for the helium plasma at  $P = 100$  MPa from the Reaction Ensemble Monte Carlo simulations of this work. The simulation uncertainties are given in the last digits as subscripts. The last column gives the left-hand side of Eq. (3.8).

$T$ (K)	$u^e$ (kJ mol $^{-1}$ )	$v$ (m $^3$ mol $^{-1}$ )	$y_{\text{He}}$	$y_{\text{He}^+}$	$y_{\text{He}^{++}}$	$y_{e^-}$	$n_t$	$6\left(\frac{\lambda_D}{a}\right)^3$
20 000	-4.58 <sub>185</sub>	0.001 662 <sub>11</sub>	0.9780 <sub>4</sub>	0.0078 <sub>2</sub>	0.0022 <sub>0</sub>	0.0120 <sub>2</sub>	1.012 <sub>0</sub>	253.74
22 500	-8.28 <sub>56</sub>	0.001 862 <sub>10</sub>	0.9465 <sub>7</sub>	0.0236 <sub>3</sub>	0.0021 <sub>0</sub>	0.0278 <sub>3</sub>	1.029 <sub>0</sub>	106.00
25 000	-12.66 <sub>147</sub>	0.002 051 <sub>16</sub>	0.8857 <sub>14</sub>	0.0541 <sub>7</sub>	0.0021 <sub>0</sub>	0.0581 <sub>7</sub>	1.062 <sub>1</sub>	45.49
27 500	-22.29 <sub>201</sub>	0.002 211 <sub>9</sub>	0.7892 <sub>13</sub>	0.1026 <sub>7</sub>	0.0018 <sub>0</sub>	0.1064 <sub>7</sub>	1.119 <sub>1</sub>	22.70
30 000	-35.14 <sub>180</sub>	0.002 348 <sub>24</sub>	0.6635 <sub>20</sub>	0.1656 <sub>10</sub>	0.0018 <sub>0</sub>	0.1691 <sub>10</sub>	1.204 <sub>1</sub>	13.41
32 500	-49.93 <sub>197</sub>	0.002 474 <sub>13</sub>	0.5273 <sub>21</sub>	0.2339 <sub>10</sub>	0.0016 <sub>0</sub>	0.2372 <sub>10</sub>	1.311 <sub>2</sub>	9.40
35 000	-63.80 <sub>162</sub>	0.002 606 <sub>19</sub>	0.4001 <sub>16</sub>	0.2977 <sub>8</sub>	0.0015 <sub>0</sub>	0.3007 <sub>8</sub>	1.430 <sub>2</sub>	7.57
37 500	-74.87 <sub>162</sub>	0.002 760 <sub>28</sub>	0.2940 <sub>16</sub>	0.3509 <sub>8</sub>	0.0014 <sub>0</sub>	0.3537 <sub>8</sub>	1.547 <sub>2</sub>	6.78
40 000	-81.22 <sub>131</sub>	0.002 934 <sub>16</sub>	0.2129 <sub>12</sub>	0.3915 <sub>6</sub>	0.0014 <sub>0</sub>	0.3942 <sub>6</sub>	1.651 <sub>2</sub>	6.55
42 500	-85.22 <sub>155</sub>	0.003 113 <sub>23</sub>	0.1541 <sub>10</sub>	0.4208 <sub>5</sub>	0.0014 <sub>0</sub>	0.4237 <sub>5</sub>	1.735 <sub>2</sub>	6.64
45 000	-84.82 <sub>161</sub>	0.003 356 <sub>46</sub>	0.1123 <sub>13</sub>	0.4414 <sub>6</sub>	0.0017 <sub>1</sub>	0.4446 <sub>7</sub>	1.801 <sub>2</sub>	6.98
50 000	-82.67 <sub>157</sub>	0.003 781 <sub>46</sub>	0.0626 <sub>7</sub>	0.4641 <sub>4</sub>	0.0031 <sub>2</sub>	0.4702 <sub>4</sub>	1.888 <sub>1</sub>	7.94
55 000	-80.43 <sub>225</sub>	0.004 222 <sub>84</sub>	0.0374 <sub>7</sub>	0.4696 <sub>6</sub>	0.0078 <sub>4</sub>	0.4852 <sub>4</sub>	1.943 <sub>2</sub>	9.11
60 000	-81.07 <sub>246</sub>	0.004 606 <sub>32</sub>	0.0239 <sub>3</sub>	0.4596 <sub>7</sub>	0.0189 <sub>5</sub>	0.4976 <sub>3</sub>	1.990 <sub>1</sub>	10.11
65 000	-89.69 <sub>495</sub>	0.005 021 <sub>27</sub>	0.0157 <sub>2</sub>	0.4300 <sub>14</sub>	0.0414 <sub>9</sub>	0.5129 <sub>5</sub>	2.056 <sub>2</sub>	10.71
70 000	-96.55 <sub>477</sub>	0.005 384 <sub>54</sub>	0.0103 <sub>2</sub>	0.3821 <sub>16</sub>	0.0752 <sub>11</sub>	0.5324 <sub>6</sub>	2.138 <sub>4</sub>	10.80
75 000	-109.9 <sub>64</sub>	0.005 939 <sub>139</sub>	0.0065 <sub>19</sub>	0.3154 <sub>24</sub>	0.1209 <sub>17</sub>	0.5572 <sub>9</sub>	2.260 <sub>5</sub>	10.67
80 000	-114.2 <sub>61</sub>	0.006 248 <sub>10</sub>	0.0042 <sub>1</sub>	0.2495 <sub>20</sub>	0.1656 <sub>14</sub>	0.5807 <sub>7</sub>	2.385 <sub>4</sub>	10.44
85 000	-121.0 <sub>57</sub>	0.006 522 <sub>105</sub>	0.0027 <sub>1</sub>	0.1904 <sub>13</sub>	0.2055 <sub>9</sub>	0.6014 <sub>5</sub>	2.509 <sub>3</sub>	10.39
90 000	-118.7 <sub>52</sub>	0.007 092 <sub>127</sub>	0.0018 <sub>0</sub>	0.1392 <sub>13</sub>	0.2399 <sub>10</sub>	0.6191 <sub>5</sub>	2.626 <sub>3</sub>	10.75
95 000	-123.2 <sub>48</sub>	0.007 467 <sub>99</sub>	0.0014 <sub>0</sub>	0.1027 <sub>11</sub>	0.2644 <sub>8</sub>	0.6315 <sub>4</sub>	2.715 <sub>3</sub>	11.23
100 000	-116.5 <sub>42</sub>	0.007 799 <sub>58</sub>	0.0011 <sub>0</sub>	0.0771 <sub>5</sub>	0.2816 <sub>4</sub>	0.6402 <sub>2</sub>	2.779 <sub>1</sub>	11.87

TABLE V. The excess molar internal energy  $u^e$ , molar volume  $v$ , mole fractions  $\{y_{\text{He}}, y_{\text{He}^+}, y_{\text{He}^{++}}, y_{e^-}\}$ , and the number of moles per total molar amount of He,  $n_t$ , for the helium plasma at  $P=400$  MPa from the Reaction Ensemble Monte Carlo simulations of this work. The simulation uncertainties are given in the last digits at subscripts. The last column gives the left-hand side of Eq. (3.8).

$T$ (K)	$u^e$ (kJ mol $^{-1}$ )	$v$ (m $^3$ mol $^{-1}$ )	$y_{\text{He}}$	$y_{\text{He}^+}$	$y_{\text{He}^{++}}$	$y_{e^-}$	$n_t$	$6\left(\frac{\lambda_D}{a}\right)^3$
20 000	-7.04 <sub>47</sub>	0.000 417 6 <sub>20</sub>	0.9839 <sub>4</sub>	0.0049 <sub>2</sub>	0.0021 <sub>0</sub>	0.0091 <sub>2</sub>	1.009 <sub>0</sub>	183.50
22 500	-9.44 <sub>94</sub>	0.000 467 2 <sub>19</sub>	0.9641 <sub>10</sub>	0.0148 <sub>5</sub>	0.0021 <sub>0</sub>	0.0190 <sub>5</sub>	1.019 <sub>1</sub>	89.57
25 000	-14.52 <sub>107</sub>	0.000 514 3 <sub>52</sub>	0.9207 <sub>13</sub>	0.0366 <sub>6</sub>	0.0020 <sub>0</sub>	0.0407 <sub>6</sub>	1.043 <sub>1</sub>	38.30
27 500	-24.92 <sub>197</sub>	0.000 549 9 <sub>28</sub>	0.8452 <sub>17</sub>	0.0745 <sub>8</sub>	0.0019 <sub>0</sub>	0.0784 <sub>8</sub>	1.085 <sub>1</sub>	17.70
30 000	-45.08 <sub>216</sub>	0.000 574 8 <sub>49</sub>	0.7374 <sub>22</sub>	0.1285 <sub>11</sub>	0.0019 <sub>0</sub>	0.1322 <sub>11</sub>	1.153 <sub>1</sub>	9.54
32 500	-70.98 <sub>155</sub>	0.000 592 8 <sub>23</sub>	0.6114 <sub>19</sub>	0.1917 <sub>10</sub>	0.0018 <sub>0</sub>	0.1951 <sub>10</sub>	1.243 <sub>1</sub>	6.14
35 000	-98.41 <sub>180</sub>	0.000 609 1 <sub>25</sub>	0.4888 <sub>18</sub>	0.2532 <sub>9</sub>	0.0016 <sub>1</sub>	0.2564 <sub>9</sub>	1.345 <sub>2</sub>	4.64
37 500	-121.1 <sub>15</sub>	0.000 629 7 <sub>24</sub>	0.3846 <sub>21</sub>	0.3054 <sub>10</sub>	0.0015 <sub>0</sub>	0.3085 <sub>10</sub>	1.446 <sub>2</sub>	3.97
40 000	-137.7 <sub>19</sub>	0.000 659 0 <sub>25</sub>	0.3020 <sub>17</sub>	0.3467 <sub>8</sub>	0.0015 <sub>0</sub>	0.3498 <sub>8</sub>	1.538 <sub>2</sub>	3.71
42 500	-147.5 <sub>17</sub>	0.000 696 9 <sub>25</sub>	0.2386 <sub>14</sub>	0.3782 <sub>7</sub>	0.0017 <sub>0</sub>	0.3815 <sub>7</sub>	1.617 <sub>2</sub>	3.67
45 000	-152.2 <sub>18</sub>	0.000 750 6 <sub>92</sub>	0.1900 <sub>16</sub>	0.4022 <sub>8</sub>	0.0019 <sub>0</sub>	0.4059 <sub>8</sub>	1.684 <sub>2</sub>	3.78
50 000	-154.4 <sub>15</sub>	0.000 844 7 <sub>41</sub>	0.1249 <sub>8</sub>	0.4329 <sub>4</sub>	0.0031 <sub>1</sub>	0.4391 <sub>4</sub>	1.783 <sub>1</sub>	4.16
55 000	-151.9 <sub>29</sub>	0.000 954 6 <sub>6</sub>	0.0853 <sub>7</sub>	0.4476 <sub>6</sub>	0.0065 <sub>4</sub>	0.4606 <sub>5</sub>	1.854 <sub>3</sub>	4.70
60 000	-152.0 <sub>23</sub>	0.001 060 <sub>4</sub>	0.0603 <sub>4</sub>	0.4497 <sub>6</sub>	0.0134 <sub>4</sub>	0.4766 <sub>3</sub>	1.911 <sub>1</sub>	5.25
65 000	-156.7 <sub>30</sub>	0.001 162 <sub>5</sub>	0.0436 <sub>4</sub>	0.4395 <sub>8</sub>	0.0258 <sub>6</sub>	0.4911 <sub>4</sub>	1.965 <sub>2</sub>	5.72
70 000	-164.5 <sub>49</sub>	0.001 265 <sub>5</sub>	0.0319 <sub>3</sub>	0.4166 <sub>11</sub>	0.0450 <sub>8</sub>	0.5065 <sub>5</sub>	2.027 <sub>2</sub>	6.05
75 000	-177.1 <sub>56</sub>	0.001 353 <sub>5</sub>	0.0233 <sub>3</sub>	0.3810 <sub>14</sub>	0.0716 <sub>9</sub>	0.5241 <sub>5</sub>	2.102 <sub>2</sub>	6.18
80 000	-188.5 <sub>61</sub>	0.001 449 <sub>23</sub>	0.0170 <sub>3</sub>	0.3370 <sub>16</sub>	0.1030 <sub>12</sub>	0.5430 <sub>7</sub>	2.189 <sub>3</sub>	6.24
85 000	-204.4 <sub>75</sub>	0.001 539 <sub>10</sub>	0.0118 <sub>2</sub>	0.2861 <sub>15</sub>	0.1387 <sub>11</sub>	0.5634 <sub>6</sub>	2.291 <sub>3</sub>	6.22
90 000	-211.5 <sub>60</sub>	0.001 627 <sub>7</sub>	0.0083 <sub>1</sub>	0.2388 <sub>13</sub>	0.1714 <sub>9</sub>	0.5815 <sub>5</sub>	2.389 <sub>3</sub>	6.27
95 000	-213.3 <sub>50</sub>	0.001 763 <sub>33</sub>	0.0057 <sub>2</sub>	0.1950 <sub>18</sub>	0.2014 <sub>13</sub>	0.5979 <sub>7</sub>	2.487 <sub>4</sub>	6.47
100 000	-216.9 <sub>59</sub>	0.001 838 <sub>14</sub>	0.0040 <sub>1</sub>	0.1590 <sub>11</sub>	0.2260 <sub>7</sub>	0.6110 <sub>4</sub>	2.570 <sub>3</sub>	6.66

Exp-6 coefficients by the polarizabilities,  $\alpha_{\text{He}}$  and  $\alpha_{\text{He}^+}$ , and by the ionization potentials,  $\text{IP}_1$  and  $\text{IP}_2$ , using

$$B_{\text{He}^+} = B_{\text{He}} \left( \frac{\text{IP}_2}{\text{IP}_1} \right)^{1/2}, \quad C_{\delta_{\text{He}^+}} = C_{\delta_{\text{He}}} \frac{\text{IP}_2 \alpha_{\text{He}^+}^2}{\text{IP}_1 \alpha_{\text{He}}^2}. \quad (4.5)$$

In Eq. (4.5),  $\alpha_{\text{He}} = 0.204\,956 \text{ \AA}^3$ ,  $\alpha_{\text{He}^+} = 0.041\,85 \text{ \AA}^3$ ,  $\text{IP}_1 = 24.587\,41 \text{ eV}$ , and  $\text{IP}_2 = 54.417\,78 \text{ eV}$ .<sup>22</sup> The final step is to calculate Exp-6 potential parameters for the He–He $^+$  interaction using the Lorentz–Berthelot rule<sup>12</sup> for combining the He–He potential and the hypothetical He $^+$ –He $^+$  potential described above. Numerical values of the Exp-6 potential parameters for the resulting He–He $^+$  intermolecular potential are listed in Table II.

The He $^{++}$  particles are essentially helium nuclei and their diameters are approximately  $10^{-4}$  times of the atomic diameters.<sup>1</sup> Hence, we considered the He $^{++}$  particles to be charged point masses that do not interact with the neutral particles. For the He–He $^{++}$  and He– $e^-$  interactions, we incorporated a temperature-dependent hard-core exclusion. The diameter of the He core was determined from the Exp-6 potential, representing the He–He interactions by means of the hybrid Barker–Henderson expression<sup>23</sup>

$$\sigma(T) = r_c + \int_{r_c}^{r_m} \left\{ 1 - \exp \left[ - \frac{u_{11}(r) + \varepsilon}{k_B T} \right] \right\} dr. \quad (4.6)$$

## V. COMPUTATIONAL DETAILS

In the REMC simulations, we used between 500 and 1400 particles in a cubic simulation box, the minimum image convention, periodic boundary conditions, and cutoff radius equal to half the box length. The Exp-6 long-range correc-

tion for the configurational energy was included,<sup>12</sup> assuming that the radial distribution function is unity beyond the cutoff radius. We treated the long-range interactions in the Deutsch potential by the reaction-field method<sup>24</sup> with the reaction-field dielectric constant set to infinity. The REMC simulations were organized in cycles as follows. Each cycle consisted of three steps:  $n_D$  particle moves,  $n_V$  volume moves, and  $n_\xi$  forward and reverse reaction moves. The three types of moves were selected at random with fixed probabilities, chosen so that the ratio  $n_D:n_V:n_\xi$  in the cycle was  $\bar{N}:1:\bar{N}$ , where  $\bar{N}$  was about 10 to 20% greater than the maximum number of particles during a simulation run. Acceptance ratios for particles moves and for volume changes were adjusted to approximately 30%.

We incorporated the IP lowering into our simulations using an iterative approach as follows. We first employed an initial simulation period, which was divided into several blocks, typically 500 cycles for equilibration and 2000 cycles for the accumulation of ensemble averages. In the first block, the REMC simulation was performed without IP lowering. After each block was completed, the composition  $\{N_i\}$  and volume  $V$  were used to calculate the effect of the IP lowering on  $\Gamma_1$  and  $\Gamma_2$ , and the pressure was set to  $P - P^{\text{IPL}}$ , with  $P^{\text{IPL}}$  given by Eq. (3.12) for a simulation in the subsequent block. The initial simulation period was terminated when the changes in  $\Gamma_1$ ,  $\Gamma_2$ , and  $P^{\text{IPL}}$  between two subsequent blocks were less than 1%; this typically occurred after three blocks. After this initial period, we generated  $2 \times 10^4$  cycles to accumulate averages of the desired quantities. The precisions of the simulated data were obtained using block averages, with 500 cycles per block. In addition to ensemble averages

of the quantities of direct interest, we also monitored convergence profiles of the thermodynamic quantities, in order to keep the development of the system under control.<sup>25</sup>

Other and potentially more efficient strategies are possible for incorporating the IP lowering. For example, it can be directly incorporated into the reaction transition probabilities of Eqs. (2.8) and (2.9), using either instantaneous values of  $\lambda_D$  in Eq. (3.6) or using values obtained from running averages of  $\{N_i\}$  and  $V$ . However, these approaches, in contrast to the iterative approach we employed, do not satisfy the condition of microscopic reversibility. Nevertheless, we observed that the REMC simulations using all approaches gave essentially identical numerical results.

For the IG and DH calculations, we numerically solved the equilibrium conditions.<sup>2,6,17</sup>

## VI. RESULTS AND DISCUSSION

We performed REMC simulations at three pressures:  $P = \{10, 100, 400\}$  MPa, and for temperatures ranging from 20 000 K to 100 000 K with temperature steps of 2500 K and 5000 K. Our REMC simulation results are summarized in Tables III–V. The last columns of these tables show that the inequality of Eq. (3.8) is satisfied, justifying our use of the IP lowering given by Eq. (3.6). Figures 1–5 show, respectively, comparisons of the simulated compositions, molar enthalpies, molar volumes, molar heat capacities, and coefficients of cubic expansion with values obtained using the IG and the DH approximations.

The subfigures of Fig. 1 show similar trends, which are most marked at the highest pressure. The IG approximation predicts compositions that indicate lower overall ionization than either the DH or the simulation values. The DH approximation slightly underpredicts the extent of ionization, but generally agrees very well with the simulation results, even at the highest pressure.

In Fig. 2, we compare the molar enthalpy,  $h$ , evaluated from the simulation data with those obtained using the IG and the DH approaches. The simulation molar enthalpy was computed as the sum of the ideal part,  $h^0$ , and the excess part,  $h^e$ ,

$$h = h^0 + h^e, \quad (6.1)$$

where

$$h^0 = \sum_i y_i h_i^0, \quad (6.2)$$

$$h^e = u^e + h^{\text{IPL}} + PV - RT. \quad (6.3)$$

$h_i^0$  is given by Eq. (3.2),  $u^e$  is the molar excess internal energy, calculated directly in the simulations, and<sup>6,17</sup>

$$h^{\text{IPL}} = -\frac{e^2 N_A}{6\pi\epsilon_0\lambda_D} \sum_{z_i > 0} y_i z_i (z_i + 1) = -\frac{e^2 N_A}{6\pi\epsilon_0\lambda_D} (2y_2 + 6y_3). \quad (6.4)$$

Figure 2 shows that the approximate results agree well with the simulation values at the lowest pressures, and the IG accuracy deteriorates slightly at 100 MPa. At 400 MPa, the

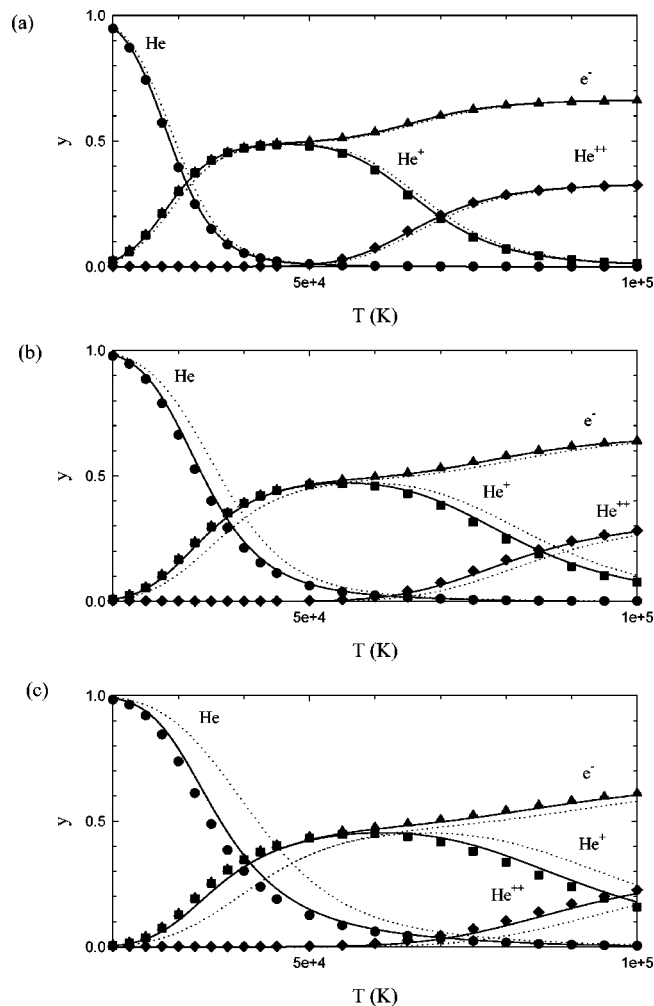


FIG. 1. Equilibrium composition of the helium plasma at (a)  $P=10$  MPa, (b)  $P=100$  MPa and (c)  $P=400$  MPa, over the temperature range 20 000 K–100 000 K. Filled symbols denote the Reaction Ensemble Monte Carlo simulation results of this work, and dotted and solid curves correspond to the results obtained using the ideal-gas and Debye–Hückel approximations, respectively.

IG approximation is poor, and the DH results are only slightly inaccurate. In all cases, the DH results lie intermediate to the IG and the simulation results.

The molar volumes of Fig. 3 show similar trends to the molar enthalpy results, but the differences are slightly greater.

The temperature derivatives of the molar enthalpy and the molar volume may be calculated essentially exactly within the IG and the DH approximations.<sup>2,6,17</sup> The former is the molar heat capacity

$$c_p = \frac{1}{n_t} \left[ \frac{\partial(n_t h)}{\partial T} \right]_{P, \text{eq}} \quad (6.5)$$

and the latter is the coefficient of cubic expansion

$$\beta = \left[ \frac{\partial \ln(n_t v)}{\partial T} \right]_{P, \text{eq}}, \quad (6.6)$$

where  $n_t$  is the total number of moles. We calculated  $c_p$  and  $\beta$  from the simulation results by numerical differentiation, performed with aid of the TableCurve™ 2D software

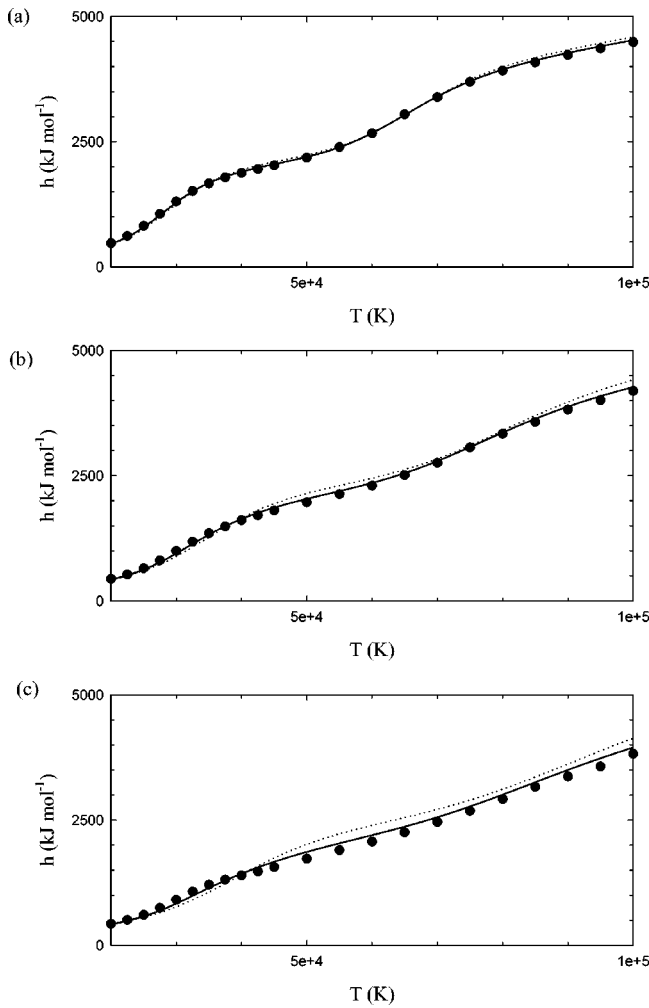


FIG. 2. Molar enthalpy of the helium plasma at (a)  $P=10$  MPa, (b)  $P=100$  MPa, and (c)  $P=400$  MPa, over the temperature range 20 000 K–100 000 K. Filled symbols denote the Reaction Ensemble Monte Carlo simulation results of this work, and dotted and solid curves correspond to the results obtained using the ideal-gas and Debye–Hückel approximations, respectively.

package.<sup>26</sup> To check the accuracy of this approach, we performed the same calculations using the DH enthalpies and volumes at the simulated temperatures, and compared them with exact analytical calculations. We found that the  $c_p$  and  $\beta$  values obtained in this way agreed with the exact  $c_p$  and  $\beta$  values to within 1%.

Comparisons of  $c_p$  and  $\beta$  obtained by numerical differentiation of the simulation data with  $c_p$  and  $\beta$  obtained from the IG and DH approaches are plotted in Figs. 4 and 5, respectively. Since  $c_p$  and  $\beta$  are derivatives of the curves of Figs. 2 and 3, the differences among the results are greater, especially at the higher pressures. In all cases, it continues to hold that the DH results lie intermediate between the IG and the simulation results. The discrepancies for the  $c_p$  results are greater than those for  $\beta$ ; at 400 MPa, the DH results are in error by up to 40%.

We evaluated the effect of the short-ranged interactions in our plasma model as described in Sec. IV by performing REMC simulations using a model with these interactions switched off. This corresponds exactly to the underlying in-

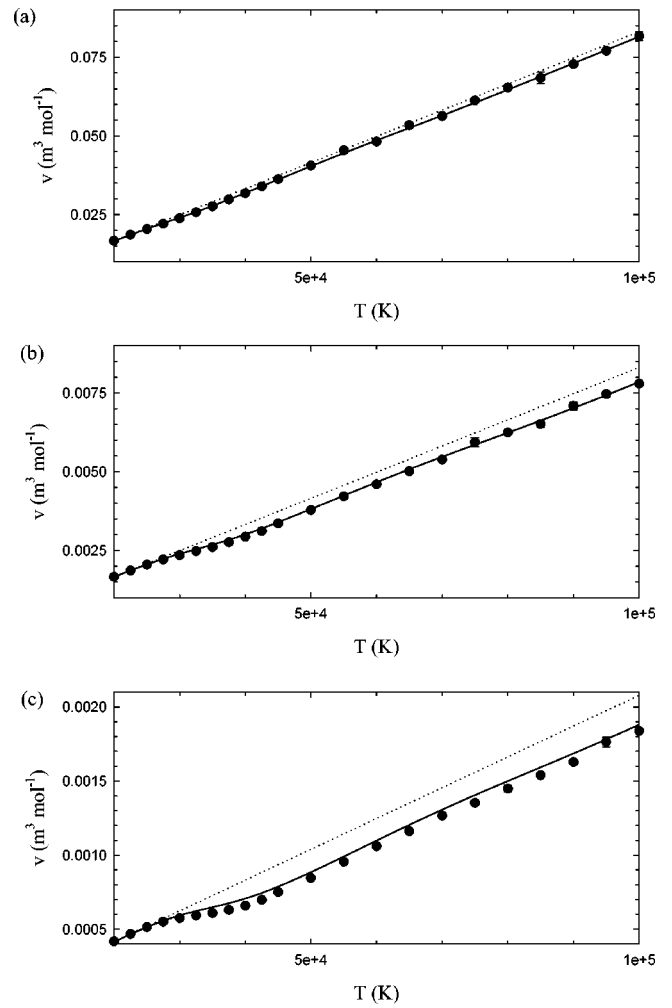


FIG. 3. Molar volume of the helium plasma at (a)  $P=10$  MPa, (b)  $P=100$  MPa, and (c)  $P=400$  MPa, over the temperature range 20 000 K–100 000 K. Filled symbols denote the Reaction Ensemble Monte Carlo simulation results of this work, and dotted and solid curves correspond to the results obtained using the ideal-gas and Debye–Hückel approximations, respectively.

termolecular potential model used by the classical DH macroscopic model. We found that the effect is nearly negligible (within the range of the simulation statistical uncertainties). However, we expect that the effect of the short-ranged interactions on the plasma properties will be important at higher densities and for plasmas containing molecular species.

We evaluated the effects of IP lowering by calculating the contributions to the pressure and to the molar enthalpy for our simulation results due separately to IP lowering and to the Coulombic forces. The IP-lowering contributions are given by Eqs. (3.12) and (6.4); the Coulombic contribution to the pressure is

$$P^{\text{Coul}} = P - \frac{RT}{v} - P^{\text{IPL}} \quad (6.7)$$

and the Coulombic contribution to the molar enthalpy is

$$h^{\text{Coul}} = h^e - h^{\text{IPL}}. \quad (6.8)$$

Figure 6 shows the contributions of the IP lowering and of the Coulombic forces to the pressure and to the molar

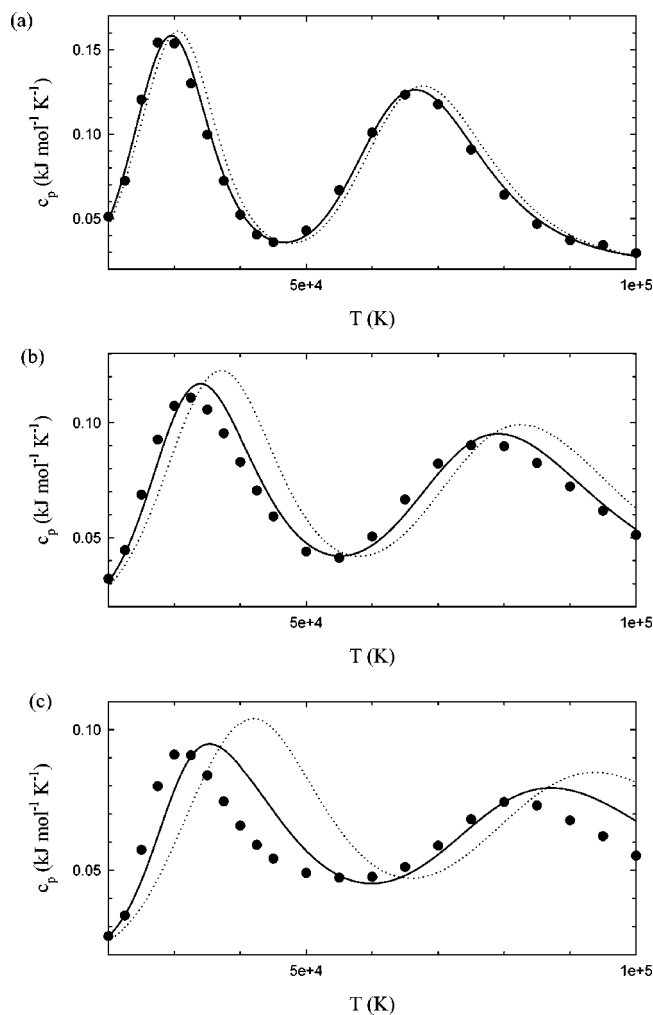


FIG. 4. Molar heat capacity of the helium plasma at (a)  $P=10$  MPa, (b)  $P=100$  MPa, and (c)  $P=400$  MPa, over the temperature range 20 000 K–100 000 K. Filled symbols denote the Reaction Ensemble Monte Carlo simulation results of this work, and dotted and solid curves correspond to the results obtained using the ideal-gas and Debye–Hückel approximations, respectively.

enthalpy at the highest pressure considered. At low temperatures, where there is only a small degree of ionization, the DH results are similar to the simulation results. Figure 6(a) shows that the DH results agree reasonably well with the simulation results for the contribution to the pressure due to IP lowering, and the DH results are less accurate for the contribution due to the Coulombic forces. For the molar enthalpy [Fig. 6(b)], the discrepancies are similar for the contributions due to both sources.

The IP-lowering contributions for the DH and the simulation approaches both arise from the same source, Eq. (3.10). Differences in these results arise only from differences in the compositions obtained using each approach. In order to more clearly indicate the accuracy of the DH theory with respect to its treatment of Coulombic forces, we show in Fig. 7 calculations at  $P=400$  MPa that exclude IP lowering (and also the short-ranged interactions). These results indicate only the effects of the Coulombic forces. It is seen that the DH theory underestimates the magnitude of the Coulombic contributions to both the pressure and to the molar

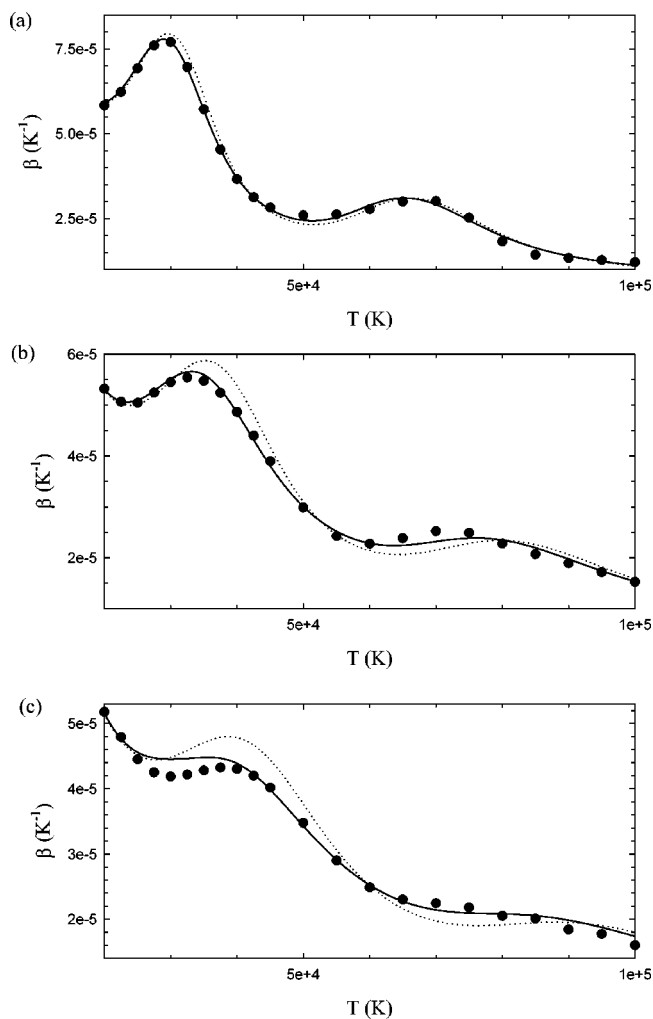


FIG. 5. Coefficient of cubic expansion of the helium plasma at (a)  $P=10$  MPa, (b)  $P=100$  MPa, and (c)  $P=400$  MPa, over the temperature range 20 000 K–100 000 K. Filled symbols denote the Reaction Ensemble Monte Carlo simulation results of this work, and dotted and solid curves correspond to the results obtained using the ideal-gas and Debye–Hückel approximations, respectively.

enthalpy. The magnitude of the DH values are  $\approx 50\%$  of the correct values.

## VII. CONCLUSIONS

We have formulated the Reaction Ensemble Monte Carlo computer simulation approach for predicting the thermodynamic properties of chemically-reacting plasmas based on a molecular-level model for the species interactions, and applied the method to the helium plasma as an example. We compared the essentially exact simulation results with those obtained from the ideal-gas (IG) and the Debye–Hückel (DH) approximations. We calculated plasma compositions, molar enthalpies, molar volumes, molar heat capacities and coefficients of cubic expansion. We also evaluated the contributions of different aspects of the model to the calculated thermodynamic properties.

At lower pressures, we generally found the DH theory to be quite accurate, and its accuracy to deteriorate with increasing pressure. We also found the IG approximation to be

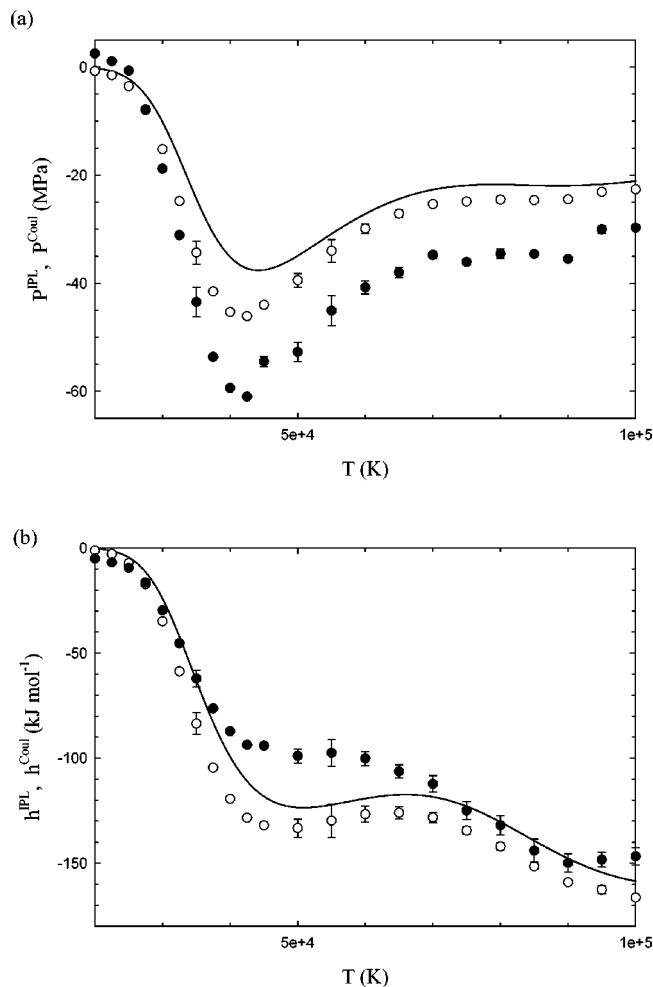


FIG. 6. Contributions of ionization-potential (IP) lowering and of the Coulombic forces for the helium plasma at  $P=400$  Mpa, over the temperature range 20 000 K–100 000 K. (a) Contributions to the total pressure and (b) contributions to the molar enthalpy. Open and filled circles denote the Reaction Ensemble Monte Carlo simulation results of this work for the IP-lowering and Coulombic contributions, respectively. The solid curve corresponds to the Debye–Hückel approximation for both the IP-lowering and the Coulombic contributions (which are identical in the case of the helium plasma).

quite good at the lower pressures, but its accuracy is less than the DH theory and also deteriorates with increasing pressure. In general, the DH and IG approximations both underpredict the degree of ionization of the helium plasma. For the properties studied, the approximations are least accurate for the molar heat capacity and the coefficient of cubic expansion. The DH theory gives values of the former that are in error by up to 40% at 400 MPa.

We found that the short-ranged forces are relatively unimportant for the helium plasmas studied; however, we expect that these will be important at higher densities and for systems containing molecular species. By means of the simulation approach, we are able to assess the accuracy of the DH theory with respect to its treatment of the contribution of the Coulombic forces to the thermodynamic properties. For the total system pressure and the molar enthalpy, it underestimates the contribution by up to 50% at pressure of 400 MPa for large values of temperature.

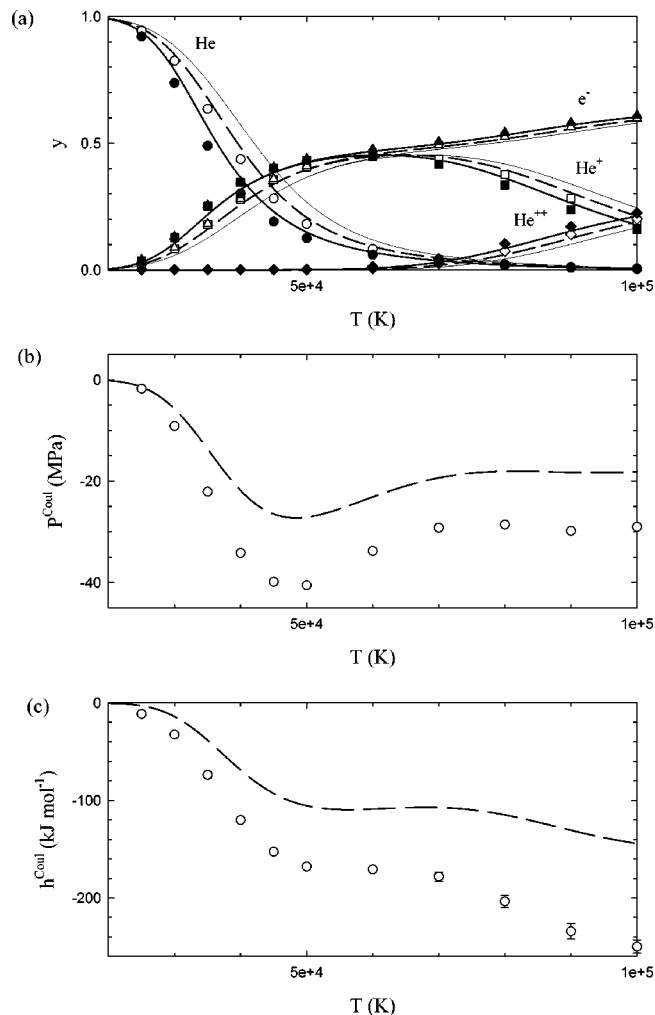


FIG. 7. Contributions of the Coulombic forces for the helium plasma at  $P=400$  MPa, over the temperature range 20 000 K–100 000 K when ionization-potential (IP) lowering is excluded from the calculations. (a) Equilibrium composition (results, including IP lowering, are shown as filled symbols and solid lines for comparison purposes only), (b) contributions of the Coulombic forces to the total pressure, and (c) contributions of the Coulombic forces to the molar enthalpy. Open symbols denote the Reaction Ensemble Monte Carlo simulation results of this work and dashed lines correspond to results obtained using the Debye–Hückel approximation.

## ACKNOWLEDGMENTS

This research was supported by the Grant Agency of the Czech Republic under Grants No. 203/98/1446 and No. 203/99/0134, and by the Natural Sciences and Engineering Research Council of Canada under Grant. No. OGP1041.

<sup>1</sup>M. I. Boulos, P. Fauchais, and E. Pfender, *Thermal Plasmas: Fundamentals and Applications* (Plenum, New York, 1994), Vol. 1.

<sup>2</sup>G. Speckhöfer, R. Gilles, W. R. Smith, and M. Bureš, in *Proceedings of the 14th International Symposium on Plasma Chemistry* (Institute for Plasma Physics, Prague, Czech Republic, 1999).

<sup>3</sup>W. R. Smith and R. W. Missen, *Chemical Reaction Equilibrium Analysis: Theory and Algorithms* (Wiley–Interscience, New York, 1982; reprinted with corrections, Krieger, Malabar, FL, 1991).

<sup>4</sup>B. Chervy, H. Riad, and A. Gleizes, *IEEE Trans. Plasma Sci.* **24**, 198 (1996).

<sup>5</sup>O. Coufal, *J. Phys. D* **31**, 2025 (1998).

<sup>6</sup>W. R. Smith, S. Gaede, M. Lísal, G. Speckhöfer, R. Gilles, and M. Bureš (in preparation).

<sup>7</sup>J.-P. Hansen, "Molecular-Dynamics Simulation of Coulomb Systems in

- Two and Three Dimensions, Molecular-Dynamics Simulation of Statistical-Mechanical Systems,” in *Proceedings of the International School of Physics*, edited by G. Ciccotti and W. G. Hoover (North-Holland, Amsterdam, 1986), pp. 89–129.
- <sup>8</sup>W. R. Smith and B. Tríska, *J. Chem. Phys.* **100**, 3019 (1994).
- <sup>9</sup>M. Lísal, I. Nezbeda, and W. R. Smith, *J. Chem. Phys.* **110**, 8597 (1999).
- <sup>10</sup>M. Lísal, W. R. Smith, and I. Nezbeda, *J. Phys. Chem. B* **103**, 10496 (1999).
- <sup>11</sup>M. Lísal, W. R. Smith, and I. Nezbeda, *AIChE. J.* **46**, 866 (2000).
- <sup>12</sup>M. P. Allen and D. J. Tildesley, *Computer Simulation of Liquids* (Clarendon, Oxford, 1987).
- <sup>13</sup>D. A. McQuarrie, *Statistical Mechanics* (Harper & Row, New York, 1976).
- <sup>14</sup>S. I. Anisimov and Yu. V. Petrov, *Tech. Phys.* **43**, 655 (1998).
- <sup>15</sup>H. R. Griem, *Phys. Rev.* **128**, 997 (1962).
- <sup>16</sup>P. Kovitya, *IEEE Trans. Plasma Sci.* **PS-13**, 587 (1985).
- <sup>17</sup>S. Gaede, “Thermodynamic Properties of High-Temperature Plasmas,” M.Sc. project, Department of Mathematics and Statistics, University of Guelph, Guelph, ON, Canada, 1999.
- <sup>18</sup>NIST Atomic Spectra Database, Energy Levels Data (<http://physics.nist.gov/PhysRefData/contents-atomic.html>).
- <sup>19</sup>H. Minoo, M. M. Gombert, and C. Deutsch, *Phys. Rev. A* **23**, 924 (1981).
- <sup>20</sup>F. H. Ree, *J. Phys. Chem.* **87**, 2846 (1983).
- <sup>21</sup>A. K. Rappé, C. J. Casewit, K. S. Colwell, W. A. Goddard III, and W. M. Skiff, *J. Am. Chem. Soc.* **114**, 10024 (1992).
- <sup>22</sup>*Handbook of Chemistry and Physics*, edited by D. R. Lide (CRC Press, Boca Raton, 1999).
- <sup>23</sup>K. E. Gubbins, W. R. Smith, M. K. Than, and E. W. Tjepel, *Mol. Phys.* **22**, 1089 (1971); W. R. Smith, in *Perturbation Theory in Classical Statistical Mechanics of Fluids*, Specialist Periodical Reports, edited by K. Singer (Chemical Society, London, 1973), Vol. 1, pp. 71–133.
- <sup>24</sup>P. Jedlovszky and G. Pálinkás, *Mol. Phys.* **84**, 217 (1995).
- <sup>25</sup>I. Nezbeda and J. Kolafa, *Mol. Simul.* **14**, 153 (1995).
- <sup>26</sup>TableCurve™ 2D, Jandel Scientific, San Rafael, CA, U.S.A.